Structural Studies of α-Bungarotoxin. 1. Sequence-Specific ^{1}H NMR Resonance Assignments†

Vladimir J. Basus,*,‡ Martin Billeter,‡,§ Robert A. Love,∥,⊥ Robert M. Stroud,∥ and Irwin D. Kuntz‡

Department of Pharmaceutical Chemistry and Department of Biochemistry and Biophysics, University of California, San Francisco, California 94143

Received July 20, 1987; Revised Manuscript Received December 8, 1987

ABSTRACT: We report the complete sequence-specific assignment of the backbone resonances and most of the side-chain resonances in the ^{1}H NMR spectrum of α-bungarotoxin by two-dimensional NMR. Problems with resonance overlap were resolved with the assistance of the HRNOESY experiment described in an accompanying paper [Basus, V. J., & Scheek, R. M. (1988) *Biochemistry* (second paper of three in this issue)]. Significant differences exist between the solution structure described here and the crystal structure of α-bungarotoxin, on the basis of the proton to proton distances obtained by nuclear Overhauser enhancement spectroscopy (NOESY) and the corresponding distances from the X-ray crystal structure [Love, R. A., & Stroud, R. M. (1986) *Protein Eng. 1*, 37]. These differences include a larger β-sheet in solution and a different orientation of the invariant tryptophan, Trp-28, making the solution structure more consistent with the crystal structure of the homologous neurotoxin α-cobratoxin. Four errors in the order of the amino acids in the primary sequence were indicated by the NMR data. These errors were confirmed by chemical means, as described in an accompanying paper [Kosen, P. A., Finer-Moore, J., McCarthy, M. P., & Basus, V. J. (1988) *Biochemistry* (third paper of three in this issue)].

Postsynaptic neurotoxins found in the venom of snakes from the Hydrophiidae and Elapidae families are potent toxins that bind tightly to nicotinic acetylcholine receptors. Through such binding, neurotoxins prevent the depolarizing action of acetylcholine on postsynaptic membranes, thus blocking neuromuscular transmission. There are two major classes of postsynaptic neurotoxins: short neurotoxins with 60–62 amino acid residues and four disulfide bonds, and long neurotoxins with 71–74 amino acid residues and five disulfide bonds. α-Bungarotoxin is a long neurotoxin containing 74 amino acid residues, and of M_r 8000, isolated from the venom of the banded krait *Bungarus multicinctus*. The structure and function of snake toxins have been extensively reviewed by Karlsson (1979), Low (1979), and Dufton and Hider (1983).

X-ray crystallographic studies of long neurotoxins have provided us with a structure for the long neurotoxin α-cobratoxin determined at 2.8-Å resolution (Walkinshaw et al., 1980) and a structure for α-bungarotoxin determined at 3.5-Å resolution (Agard & Stroud, 1982) subsequently refined to 2.5-Å resolution (Love & Stroud, 1986). Differences in the primary sequence detected by our NMR[1] assignment work were incorporated into the most recent refined X-ray structure (Kosen et al., 1988), providing the basis for comparison with the NMR-determined distance data presented here. Nuclear magnetic resonance studies have been carried out for α-cobratoxin (Kondakov et al., 1984), the results being basically in agreement with its crystal structure. Early NMR experiments on α-bungarotoxin with partial assignments (Inagaki et al., 1985) have indicated that there are genuine differences between the solution and crystal structures in the vicinity of Trp-28. Our current studies, after complete sequence-specific assignments, show that there are differences not only between the crystal and solution studies near this residue but also in other regions of the molecule, with the triple-stranded β-sheet being more extended in solution on both of its ends.

In this paper, the first of three in this issue, we present the complete sequence-specific ^{1}H NMR resonance assignments for the backbone protons of α-bungarotoxin and also the assignment of most of the side-chain proton resonances. We also present the assignment of 78 nonsequential NOEs and a comparison of the corresponding distances to those of the X-ray crystal structure. The second paper shows the application of a new two-dimensional NMR experiment for resolution of resonance overlap problems between α-protons. The third paper describes the primary sequence errors encountered in the published sequence of α-bungarotoxin (Mebs et al., 1971), as indicated by NMR data and confirmed by chemical means. The third paper also characterizes a minor isotoxin found in standard α-bungarotoxin preparations.

Materials and Methods

Isolation and purification of α-bungarotoxin is described in the third paper of this series (Kosen et al., 1988). Samples were prepared by dissolving the lyophilized powder in either

† This work was supported by Grants GM-19267 (I.D.K.), RR-01695 (I.D.K.), and GM-24485 (R.M.S.) from the National Institutes of Health and by a grant from the Academic Senate, University of California (V.J.B.). The UCSF Magnetic Resonance Laboratory was partially funded by grants from the National Science Foundation (DMB 8406826) and the National Institutes of Health (RR-01668).

* Author to whom correspondence should be addressed.

‡ Department of Pharmaceutical Chemistry.

§ Present address: Institut für Molekularbiologie und Biophysik, ETH-Hönggerberg, CH-8093 Zürich, Switzerland.

∥ Department of Biochemistry and Biophysics.

⊥ Present address: Department of Biological Sciences, University of Pittsburgh, Pittsburgh, PA 15260.

[1] Abbreviations: NMR, nuclear magnetic resonance; 2D, two dimensional; NOE, nuclear Overhauser effect; NOESY, 2D NOE spectroscopy; COSY, 2D *J*-correlated spectroscopy; HOHAHA, 2D homonuclear Hartmann–Hahn spectroscopy; HRNOESY, HOHAHA relayed coherence transfer NOE spectroscopy; TSP, sodium (trimethylsilyl)-propionate; ppm, parts per million; γ, gyromagnetic ratio; H_1, radio frequency field strength; t_1, evolution time; t_2, data acquisition time; ω_1, Fourier transformed t_1 dimension; ω_2, Fourier transformed t_2 dimension.

0006-2960/88/0427-2763$01.50/0

Table I: ^{1}H Chemical Shifts[a] and Assignments of α-Bungarotoxin at pH 4.0, 35 °C

residue	NH	C$^\alpha$H	C$^\beta$H	others	residue	NH	C$^\alpha$H	C$^\beta$H	others
Ile-1	n.o.[b]	4.17	1.87	C$^\gamma$H$_3$ 0.87; C$^\gamma$H$_2$ 1.15, 1.55; C$^\delta$H$_3$ 0.71	Cys-44	8.45	5.57	3.22, 3.00	
Val-2	8.10	4.95	1.57	C$^\gamma$H$_3$ 0.57, 0.85	Ala-45	9.39	4.58	1.40	
Cys-3	8.76	5.07	2.40, 2.97		Ala-46	8.77	4.84	1.52	
His-4	9.18	5.12	2.95, 2.67	C$^\delta$H 6.51; C$^\epsilon$H 8.14	Thr-47	7.40	4.33	3.96	C$^\gamma$H$_3$ 1.12
Thr-5	9.03	5.16	3.99	C$^\gamma$H$_3$ 1.28	Cys-48	9.00	4.55	2.91	
Thr-6	8.22	4.73	5.02	C$^\gamma$H$_3$ 1.40	Pro-49		4.15	2.10, 1.55	C$^\delta$H$_2$ 3.18; C$^\gamma$H$_2$ 1.03, 1.38
Ala-7	9.21	4.32	1.52		Ser-50	8.01	4.19	3.80, 3.75	
Thr-8	7.06	4.50	4.28	C$^\gamma$H$_3$ 1.04	Lys-51	8.30	4.32	1.95, 1.75	1.31, 1.45; C$^\epsilon$H$_2$ 3.11
Ser-9	8.25	4.58	3.78, 3.67		Lys-52	8.20	4.56	0.99	1.31, 1.36; C$^\delta$H$_2$ 1.48, 1.60; C$^\epsilon$H$_2$ 2.88
Pro-10		4.87	2.50, 2.14	C$^\gamma$H$_2$ 1.81; C$^\delta$H$_2$ 3.58					
Ile-11	8.42	4.12	1.69	C$^\gamma$H$_3$ 1.00; C$^\gamma$H$_2$ 1.87, 1.18; C$^\delta$H$_3$ 0.88	Pro-53		4.17	2.19, 1.74	
Ser-12	7.74	4.92	3.90, 3.78		Tyr-54	7.29	4.55	3.44, 3.17	C$^\epsilon$H 6.74; C$^\delta$H 7.10
Ala-13	8.29	5.12	0.92		Glu-55	7.68	5.11	2.00	C$^\gamma$H$_2$ 2.00, 1.89
Val-14	8.79	4.66	2.07	C$^\gamma$H$_3$ 0.83, 0.86	Glu-56	8.82	4.76	2.34, 2.30	C$^\gamma$H$_2$ 2.00
Thr-15	8.49	4.42	3.99	C$^\gamma$H$_3$ 1.22	Val-57	8.57	5.32	1.87	C$^\gamma$H$_3$ 0.94, 0.88
Cys-16	8.87	4.85	3.25, 3.01		Thr-58	9.03	4.76	3.99	C$^\gamma$H$_3$ 1.22
Pro-17		4.72	2.43, 1.75	C$^\gamma$H$_2$ 1.88; C$^\delta$H$_2$ 3.98, 3.49	Cys-59	9.16	5.62	3.72, 3.02	
Pro-18		4.32	1.87, 2.31	C$^\gamma$H$_2$ 1.99, 2.12; C$^\delta$H$_2$ 3.87, 3.58	Cys-60	9.19	5.12	3.59, 3.41	
Gly-19	8.77	4.26, 3.66			Ser-61	8.87	4.94	3.80, 4.19	
Glu-20	7.80	4.31	2.32, 2.19	2.03	Thr-62	7.51	4.75	4.27	C$^\gamma$H$_3$ 1.21
Asn-21	8.00	4.95	3.00, 2.65	N$^\delta$H$_2$ 6.96, 7.44	Asp-63	8.33	4.75	2.34	
Leu-22	8.25	4.99	1.69, 1.45	C$^\gamma$H 1.57; C$^\delta$H$_3$ 0.70, 0.77	Lys-64	9.93	3.14	1.01, 0.36	C$^\gamma$H$_2$ 1.52, 1.95; C$^\delta$H$_2$ 1.49, 1.53; C$^\epsilon$H$_2$ 2.65, 2.75
Cys-23	8.77	5.93	3.22, 2.86		Cys-65	7.64	4.53	3.75, 3.50	
Tyr-24	8.99	5.97	3.00, 2.65	C$^\delta$H 6.65; C$^\epsilon$H 6.74	Asn-66	8.92	4.97	2.54	N$^\delta$H$_2$ 7.53, 7.82
Arg-25	9.05	5.24	1.93	1.36, 1.50; C$^\delta$H$_2$ 3.01; N$^\epsilon$H 7.16	Pro-67		3.77	1.76, 2.11	C$^\gamma$H$_2$ 1.67, 1.84; C$^\delta$H$_2$ 3.57
Lys-26	9.76	5.74	2.09, 1.91	1.58, 160; C$^\epsilon$H$_2$ 2.55, 2.57	His-68	8.49	4.21	3.00, 2.86	C$^\delta$H 6.99; C$^\epsilon$H 8.50
Met-27	9.17	6.00	2.02, 2.48	C$^\gamma$H$_2$ 1.94; SCH$_3$ 1.97	Pro-69		4.42	2.25	C$^\gamma$H$_2$ 1.87; C$^\delta$H$_2$ 3.51, 2.86
Trp-28	8.63	5.23	3.63, 3.43	C$^\eta$H 6.87; C$^{\zeta 3}$H 7.22; C$^{\zeta 2}$H 7.22; C$^\epsilon$H 7.51; C$^\delta$H 7.04; N$^\epsilon$H 10.42	Lys-70	9.02	4.31	1.77, 1.85	C$^\gamma$H$_2$ 1.45; C$^\delta$H$_2$ 1.70; C$^\epsilon$H$_2$ 3.00
Cys-29	9.26	5.10	3.05, 3.37		Arg-71	8.29	4.63	1.87, 1.75	C$^\gamma$H$_2$ 1.68, 1.46; C$^\delta$H$_2$ 3.21; N$^\epsilon$H 7.16
Asp-30	8.35	4.84	2.73, 3.17		Gln-72	8.37	4.32	2.32, 2.04	C$^\gamma$H$_2$ 1.97
Ala-31	8.23	4.03	1.08		Pro-73		4.43	2.28	C$^\gamma$H$_2$ 2.00; C$^\delta$H$_2$ 3.78, 3.67
Phe-32	8.27	4.78	3.39, 2.95	C$^\delta$H 7.23; C$^\zeta$H 7.30; C$^\epsilon$H 7.36	Gly-74	7.95	3.80		
Cys-33	7.79	4.13	3.54, 3.19						
Ser-34	8.87	4.29	3.95, 4.02						
Ser-35	7.76	4.65	3.96, 3.90						
Arg-36	8.33	4.54	1.88, 1.95	C$^\gamma$H$_2$ 1.78, 1.65; C$^\delta$H$_2$ 3.09; N$^\epsilon$H 7.05					
Gly-37	7.71	4.30, 3.92							
Lys-38	8.16	4.20	1.48, 1.61	1.25; C$^\epsilon$H$_2$ 2.97					
Val-39	8.55	3.66	0.52	C$^\gamma$H$_3$ 0.58, 0.48					
Val-40	7.70	4.78	1.77	C$^\gamma$H$_3$ 0.58, 0.61					
Glu-41	9.38	4.98	2.29, 2.25						
Leu-42	8.76	5.07	1.52	C$^\gamma$H$_2$ 1.52; C$^\delta$H$_3$ 0.86, 0.92					
Gly-43	6.67	4.27, 4.02							

[a] Chemical shifts in ppm from internal TSP; accuracy ±0.01 ppm. [b] n.o., not observed.

H_2O (5% D_2O) or 99.96% D_2O, with a final concentration of 6–7 mM in α-bungarotoxin; 1 mM TSP was added as an internal chemical shift reference. Two-dimensional spectra were acquired between 4 and 45 °C at pH 4.0, between 10 and 55 °C at pH 4.8, and between 25 and 45 °C at pH 5.8.

Spectra were obtained on a General Electric GN-500 spectrometer. All spectra were run in the phase-sensitive mode with quadrature detection in both dimensions. NOESY spectra were acquired with the procedure of States et al. (1982). Recycle times between 2.5 and 3.5 s were used. Double-quantum filtered COSY (Piantini et al., 1982; Shaka et al., 1983; Rance et al., 1984) and HRNOESY (Basus & Scheek, 1988) spectra were acquired with time-proportional phase incrementation of the first pulse (Redfield & Kuntz, 1985; Marion & Wüthrich, 1983). HOHAHA spectra with MLEV-17 (Bax & Davis, 1985) were acquired after modification of the spectrometer by inclusion of a 6-W amplifier as a transmitter with a γH_1 of 8 kHz and with the same power for the initial 90° pulse. Mixing times from 30 to 75 ms were used. Spectra in H_2O were acquired with irradiation of the H_2O resonance during the relaxation delay. For NOESY spectra, the water resonance was also irradiated during the mixing time. The HRNOESY spectra (Basus & Scheek, 1988) were acquired with a 160-ms NOESY mixing time and a 30-ms HOHAHA relay mixing time. Spectral widths were 6024 Hz for all spectra. Phase-sensitive double-quantum filtered COSY and HRNOESY spectra were acquired with 800–1024 t_1 increments and were zero filled in t_1 to 1024 data points with 4096 points in t_2. All other spectra were acquired with 450–512 t_1 increments and zero filled in t_1 to give a final real matrix of 1024 points in ω_1 by 2048 points in ω_2. Data processing was carried out with programs initially developed at Dr. R. Kaptein's laboratory at the University of Groningen, Groningen, The Netherlands, and then adapted to work on a VAX 11/750 computer with a UNIX operating system. Program modifications and improvements were done by Dr. R. M. Scheek and Dr. S. Manogaran in our laboratory. Base-line correction was used in both dimensions for phase-sensitive spectra, being carried out in ω_2 first (Basus, 1984). The automatic base-line correction program was written by Dr. S. Manogaran and Dr. R. M. Scheek on the basis of the algorithm described by Pearson (1977). A factor of 1.4 was used between consecutive contour levels for all contour plots.

Results and Discussion

Assignment Strategy. Sequential assignments were carried out according to the established procedures of Wüthrich et al. (Wüthrich et al., 1982; Billeter et al., 1982; Wagner et al., 1982) based on the NOEs between the amide protons of one residue and the α-protons, β-protons, and amide protons of

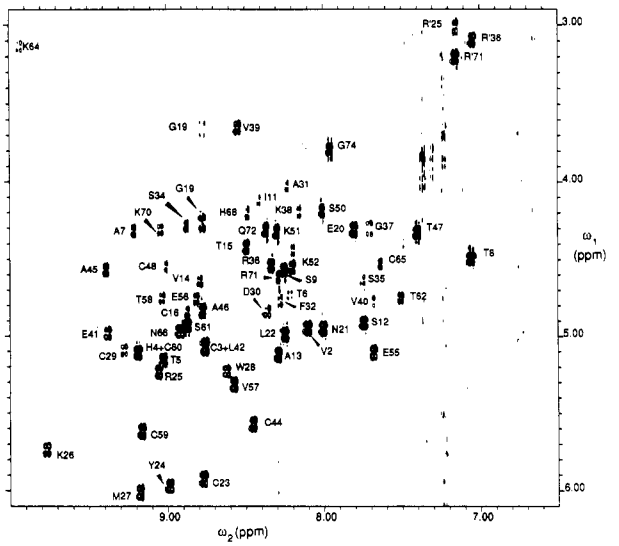

FIGURE 1: Fingerprint region of the phase-sensitive double-quantum filtered COSY spectrum of α-bungarotoxin at pH 4.0 and 35 °C, showing assignments with the single-letter code for the amino acids. The R′ cross-peaks are for the side-chain ε-NH protons of the arginines.

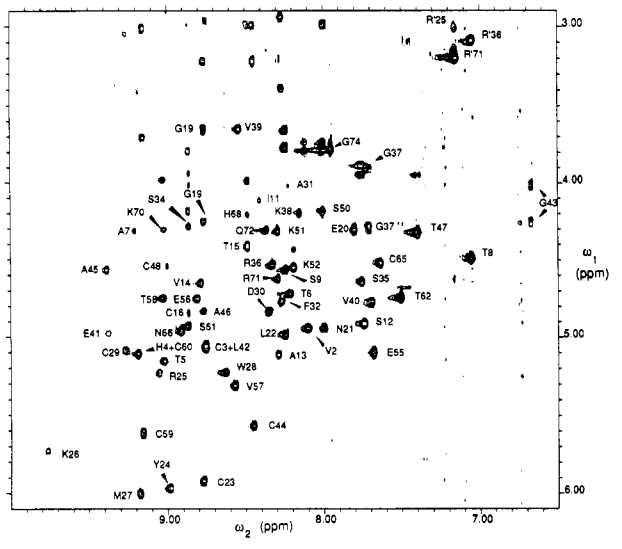

FIGURE 2: HOHAHA spectrum of α-bungarotoxin under the same conditions and in the same spectral region as in Figure 1. Only the directly coupled (not relayed) cross-peaks are labeled. The mixing time used was 70 ms.

the preceding residue (these distances are labeled $d_{\alpha N}$, $d_{\beta N}$, and d_{NN}, respectively). The results are listed in Table I.

We have adopted a computer-based approach to the problem, however, by working with peak positions. Chemical shifts and spin system connectivities for as many resonances as possible were obtained from COSY and HOHAHA experiments, as described in the next section. An arbitrary numbering scheme was adopted to label each of the spin systems observed. The NOESY cross-peak positions were then compared to those of each of the resonances observed in COSY and HOHAHA spectra, yielding assignments in each of the two dimensions to spin systems, with a discrimination of ±0.01 ppm. This criterion for comparison of the observed resonances was determined through the isolated resonances where assignment was unambiguous. With this criterion, most of the NOESY cross-peaks (about 90%) had multiple assignment possibilities in at least one of the two dimensions. Following the temperature dependence of the NOESY and COSY (or HOHAHA) cross-peaks allowed us to reduce the number of NOESY cross-peaks with multiple assignments, due to differences in the temperature dependence of the chemical shifts of each of the backbone NH protons. After making use of this differential temperature dependence, 46% of the NOESY cross-peaks in the NH to NH region had multiple assignments, while the corresponding number for the α-proton to NH region was 83%. Some of these ambiguities were resolved with the HOHAHA relayed NOESY (HRNOESY) experiment described in the second paper of this series. Finally, to improve the α-proton assignments, we used the pH dependence, by analyzing spectra run at pH 4.0, 4.8, and 5.8. At this stage, nearly all of the NOESY cross-peaks in the NH to NH region were uniquely assigned while the number of cross-peaks in the α-proton to NH region with multiple assignments was reduced to 48%.

With most of the NOESY cross-peaks assigned to the arbitrarily numbered spin systems, we then used an interactive computer program developed in our laboratory (Billeter et al., 1988) in order to obtain sequential assignments based on the rules developed in Wüthrich's laboratory (Billeter et al., 1982).

Identification of Spin Systems. Spin systems were identified to residue types on the basis of COSY, NOESY, RELAY, and HOHAHA spectra in D_2O and H_2O. Three of the four glycines could be identified on the basis of the presence of COSY cross-peaks from the NH proton to two α-protons. Figure 1 shows these cross-peaks clearly for Gly-19. In this spectrum, the second NH to α-proton connectivity for Gly-37 is not observable. It was, however, observed in COSY spectra run under different conditions and is clearly visible in the HOHAHA spectrum (Figure 2) due to relay magnetization transfer through the large α-proton to α-proton coupling (the shape of this cross-peak is somewhat distorted by the presence of large relay cross-peaks from the NH to the β-protons of Ser-35). A similar situation occurred with Gly-43. Neither of the two possible NH to α-proton connectivities are observed in the COSY spectrum (Figure 1), but they are clearly visible in the HOHAHA spectrum (Figure 2). We find that HOHAHA spectra have better sensitivity than COSY spectra. For Gly-74 the shifts of both α-protons are nearly the same. It was, however, identified as a glycine due to its triplet pattern for the NH resonance as observed in triple-quantum filtered spectra.

The three arginines were identified on the basis of their side-chain NH resonances which are coupled to the δ-protons. The HOHAHA spectra showed relayed connectivities from the NH to the γ- and β-protons for all arginines, and even to the α-proton for Arg-71. Relayed connectivities are also observed from the backbone NH to the γ- and β-protons, so that the arginines could be easily identified on the basis of these common chemical shifts. Figure 3 shows these peaks for Arg-36 and Arg-71.

Five of the six lysines were identified from a combination of HOHAHA and COSY spectra. Relay peaks were observed from the ε-protons to the δ-, γ-, β-, and even α-protons for five lysines. With the arginines already identified, and the prolines identifiable due to the lack of a backbone NH, the only other long-chain residues were those containing only α-, β-, and γ-protons in an uninterrupted coupling network (one methionine, one glutamine, and four glutamic acid residues). These residues could have at most five chemical shifts in the aliphatic region. Lysines were then identified by observation of more than five chemical shifts in a spin system not assigned to an arginine or a proline. The remaining lysine had severe overlap of its side-chain resonances and was only identified by sequential assignment to Lys-26 in the central loop of the triple-stranded β-sheet, which was possible in D_2O, and was therefore assigned very early, along with Met-27, as described

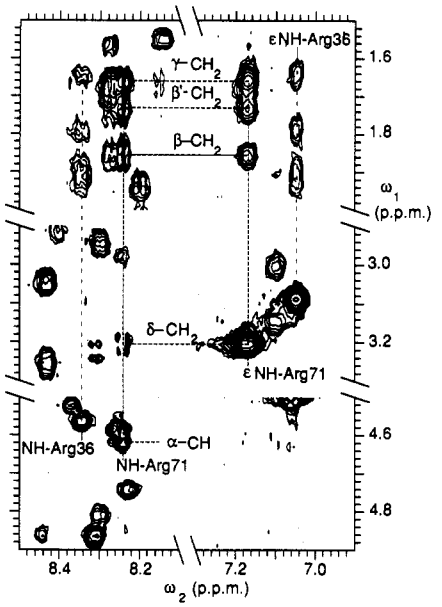

FIGURE 3: Sections of the HOHAHA spectrum of α-bungarotoxin at pH 4.8 and 35 °C, with a 70-ms mixing time. The evidence for identifying Arg-71 and Arg-36 as arginines is shown.

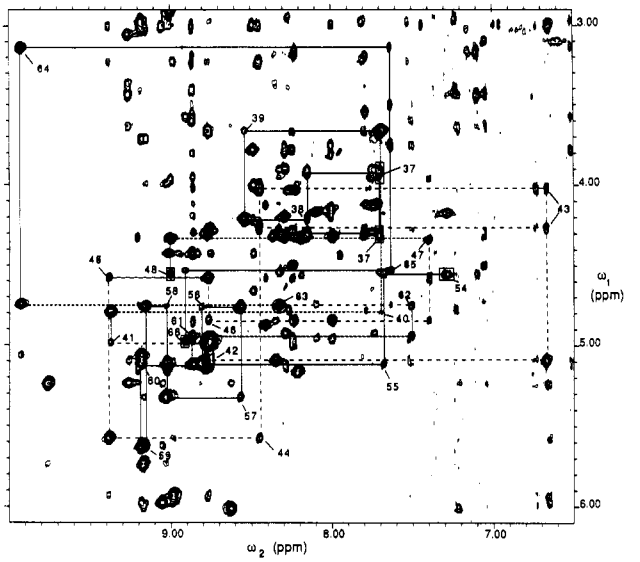

FIGURE 4: Portion of the NOESY spectrum of α-bungarotoxin in H_2O at 35 °C and pH 4.0, showing the $d_{\alpha N}$ connectivities for residues 37–48 and 54–66. Residue numbers are shown, indicating the position of the COSY cross-peaks (see Figure 1). The boxed cross-peaks indicate starting and ending points for sequential assignment. The circled cross-peak indicates the position where the COSY peak for Asp-63 would be expected. It was not observed due to negligible coupling between its NH and α-proton.

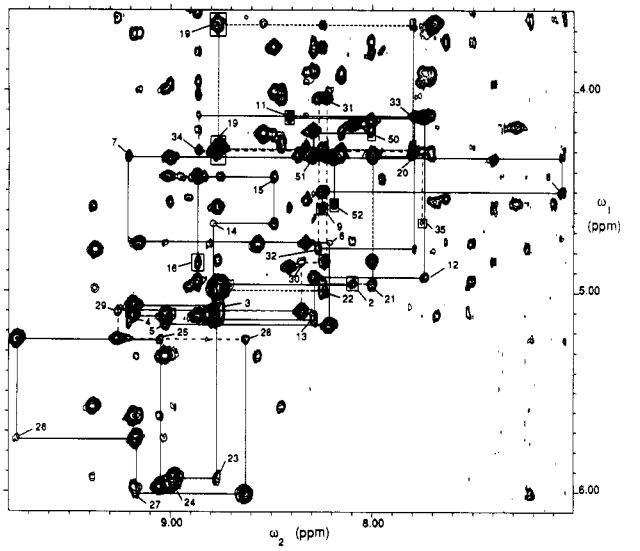

FIGURE 5: Portion of Figure 4 showing the $d_{\alpha N}$ connectivities for residues 2–9, 11–16, and 19–35. The positions of the COSY cross-peaks for residues 6 and 14 are indicated by circles. The corresponding NOESY cross-peaks were not observed due to the proximity of the H_2O resonance which is being irradiated.

in the next section. Since there is only one methionine in α-bungarotoxin, the remaining spin systems with more than three chemical shifts in the aliphatic region, and not linked to a methyl resonance, were assigned to either glutamic acid or glutamine.

Valines and leucines are easily identified by observation of COSY cross-peaks between the β-proton (γ-proton for leucines) and two methyl resonances. The five valines showed coupling from the β- to the α-proton, so that their spin systems were easily identified. Linking the methyl resonances of the two leucines to the α-protons was more difficult since the β- and γ-proton resonances are close to each other but was possible due to observation of cross-peaks between the β-protons and the methyl resonances in HOHAHA spectra, as well as cross-peaks between the α-protons and the β- and γ-protons. The two isoleucines were easily identified by their unique coupling pattern (Wider et al., 1982; Nagayama & Wüthrich, 1981).

Six of the seven threonines were readily identified from the methyl to α-proton relay cross-peaks in HOHAHA spectra. The last threonine relay cross-peak, however, was not observed. After sequential assignment of Thr-6, its NH to α-proton COSY cross-peak was identified as the one to which no relay cross-peak had been observed. Since the chemical shifts of the α- and β-protons are not so near to each other as to preclude the observation of a COSY or HOHAHA cross-peak between them, the only explanation for these observations is that the coupling constant between these protons is near zero. Since the Thr-6 spin system was not identified before sequential assignment, the alanine and threonine spin systems were grouped together for the assignment program.

The complete spin systems of the aromatic amino acid residues, excluding the histidines, were assigned by use of the NOESY cross-peaks between previously assigned aromatic resonances (Endo et al., 1981) and their β-proton resonances (Billeter et al., 1982).

Sequential Assignments. Initial assignments were aided significantly by observation of α-proton to α-proton cross-peaks in NOESY spectra in D_2O, which are characteristic of an antiparallel β-sheet. The available information from the crystal structure of α-bungarotoxin (Love & Stroud, 1982) and the homologous protein α-cobratoxin (Walkinshaw et al., 1980) shows one triple-stranded β-sheet. There are several slow-exchanging NH protons which are involved in the hydrogen bonds of this β-sheet. These were clearly observed in spectra in D_2O solution. The backbone NH protons of the central strand are all in slow exchange. Sequential assignment of this fragment (Leu-22 to Trp-28) was obtained from D_2O spectra, where all the sequential connectivities were observed. The α-proton to α-proton β-sheet NOE contacts then allowed assignment of residues in the other two strands of this β-sheet. These results were arrived at independently, from one-dimensional NOE experiments by Inagaki et al. (1985). Their assignments for Met-27 and Val-40 are in error, however, and the correct assignment, shown in Table I, is related to theirs by interchange of the chemical shifts of this pair of protons,

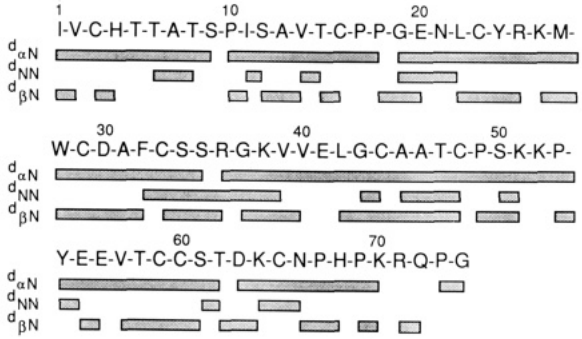

FIGURE 6: Assignment diagram for α-bungarotoxin ($d_{\alpha\delta}$ connectivities for prolines were included with the $d_{\alpha N}$ connectivities).

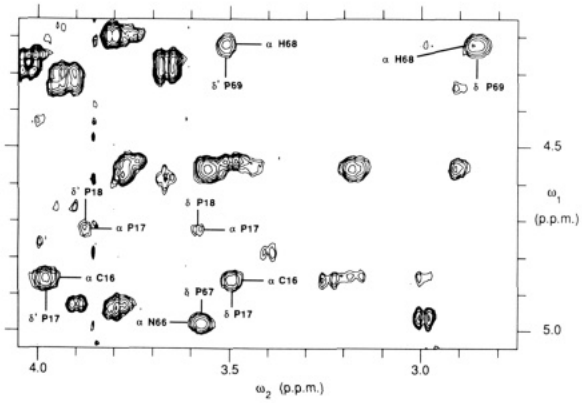

FIGURE 7: Portion of the NOESY spectrum of α-bungarotoxin in H_2O at 35 °C and pH 4.0, showing the α-proton to proline δ-proton sequential NOESY cross-peaks.

which are spatially in close proximity.

NOESY spectra in H_2O were acquired with a mixing time of 160 ms for sequential assignments. Most of the $d_{\alpha N}$ connectivities were observed and are shown in Figures 4 and 5. The assignment diagram (Figure 6) includes as $d_{\alpha N}$ the proline $d_{\alpha\delta}$ NOEs. The distance between the α-proton of residue i and one of the proline δ-protons of residue $i + 1$ is short enough to produce an NOE. These cross-peaks can be used as the $d_{\alpha N}$ cross-peaks of other amino acid residues for sequential assignments (Wüthrich et al., 1984). Of the seven missing $d_{\alpha N}$ connectivities in Figure 6, two involved proline δ-protons. The $d_{\alpha\delta}$ cross-peaks are in the very crowded region of α-proton to β-proton cross-peaks and are probably under one of these cross-peaks, thus unobservable. The $d_{\alpha\delta}$ sequential NOESY cross-peaks for four of the prolines are shown in Figure 7 at a pH of 4.0. The cross-peaks for Pro-49 and Pro-53 were not observed at this pH because of overlap problems. They were, however, observed at pH 4.8. Most of the remaining missing $d_{\alpha N}$ connectivities could be explained by overlap with another cross-peak. The HRNOESY experiment described in the second paper of this series established the connectivity between Cys-4 and His-5, as shown therein. This connectivity was difficult to detect because of the overlap between the NOESY cross-peak connecting the α-proton of Cys-4 to the NH of His-5 and the intraresidue NOESY cross-peak connecting the NH of His-5 to its α-proton. A similar situation was encountered between Thr-62 and Asp-63. In this case, however, a relayed NOESY cross-peak was not observed due to the negligible coupling between the NH and α-proton of Asp-63. The spin system of Asp-63 was only detected near the end of the assignment procedure, as a new NH chemical shift from cross-peaks in NOESY spectra only.

The assignment program (Billeter et al., 1988) uses all the NOESY cross-peaks observed, regardless of intensity. In many

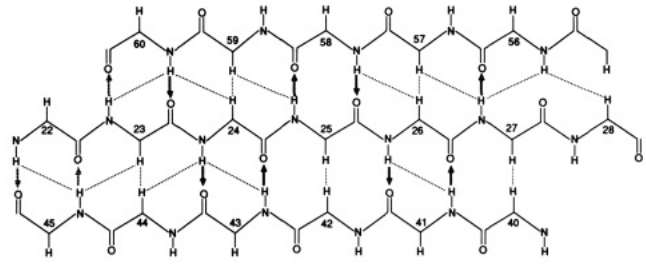

FIGURE 8: Schematic representation of the proposed β-sheet solution structure of α-bungarotoxin showing the observed NOEs from NOESY spectra in H_2O and D_2O. The solid arrows indicate the hydrogen bonds found in the crystal structure (Kosen et al., 1988). The dashed arrows indicate the additional hydrogen bonds found in solution on the basis of the amide proton exchange rates [14–94-h half-lives at 35 °C and pH 6.5 from Endo et al. (1981)] and the NOEs shown here.

cases more than one assignment of a NOESY cross-peak was possible. Multiple assignments were reduced, as much as possible, by use of the HRNOESY experiment and by varying temperature and pH. We emphasize that multiple assignments of some cross-peaks still occurred at this stage. The assignment program allows for some ambiguity. The assignment procedure then involved inspection of possible sequential NOEs. First, the presence of two sequential connectivities of the type $d_{\alpha N}$, $d_{\beta N}$, or d_{NN} (Billeter et al., 1982), based on unambiguous NOESY data, was used to establish sequential assignments. As the assignment progressed, the program automatically eliminated possibilities on the basis of the completed assignments. The next step was to continue assignments for residues adjacent to the residues already assigned. We explored residues for which there were two sequential connectivities, one of which was unambiguous and the second questionable (i.e., one of the chemical shifts of the NOESY cross-peak could be assigned to more than one spin system). This was followed by assignments based on a single unambiguous NOE, then by assignments based on two questionable NOEs, and finally assignments based on one questionable NOE. When there was more than one possible assignment to a sequential neighbor, no definite assignment was made. In such cases, assignments were pursued in other regions first. Carrying out this procedure with various starting points always led to assignment of 85% of the residues, until it was realized that a change in the published primary sequence (Mebs et al., 1971) would use the observed NOEs successfully for 100% assignment. Four errors in the sequence were detected initially in this manner and then confirmed by chemical means (Kosen et al., 1988).

The evidence for sequential assignments is summarized in Figure 6. The chemical shifts, given in Table I, are at pH 4.0 where most of the work was done.

Structure of α-Bungarotoxin in Solution. From the early stages of the assignment process, it was evident that the solution structure was different from the X-ray structure as discussed previously in reporting the crystal structure by Love and Stroud (1986). In solution, the β-sheet extends farther than in the crystal structure in the region of Trp-28, as shown in Figure 8, on the basis of the α-proton to α-proton close contacts observed in solution between Val-40 and Met-27, and the NOEs were observed between the Trp-28 ring and the Val-39 β-protons and methyl protons. In the crystal structure these protons are about 10 Å apart because the side chain of Trp-28 lies on the opposite side of the β-sheet from Val-39, or from the side found for the other neurotoxin X-ray structures. This is clearly inconsistent with the solution structure since NOEs, under the conditions of the NOESY spectra obtained here with a 160-ms mixing time, can only be observed

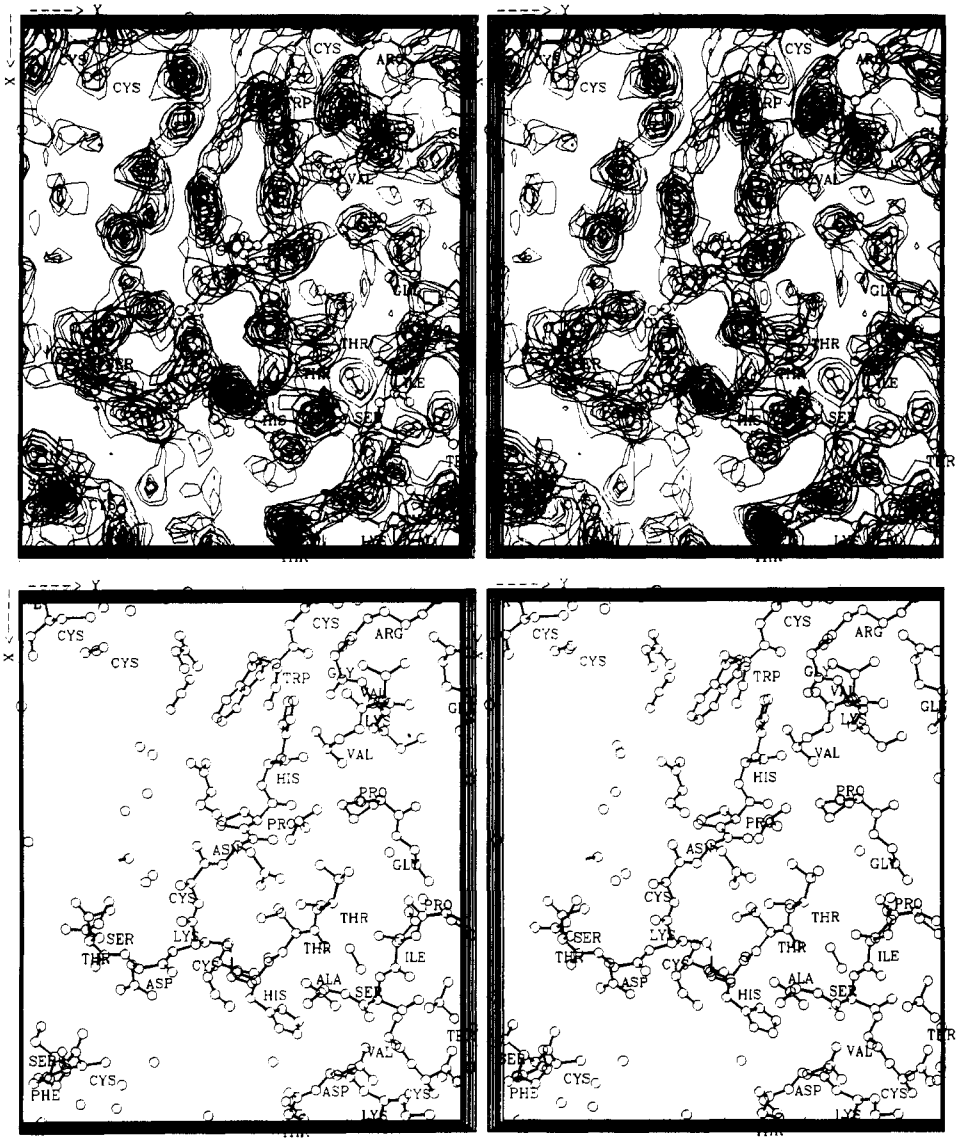

FIGURE 9: Electron density map at 2.5-Å resolution computed with amplitudes ($2F_o - F_c$), where residues 3, 4, 5, and 64–67 were omitted from the phase calculations, shown in stereo (top). The changes in the sequence (Kosen et al., 1988) at residues 9, 11, 67, and 68 were included. Below is the part of the model matching the model and density above. At the bottom is Thr-62, Asp-63, Lys-64, and Cys-65 of a neighboring molecule. Above it lies Pro-10 through Ala-13. Above that is Cys-3, His-4, Thr-5, and Thr-6 whose conformation is discussed, without bias in the density map for residues 3, 4, and 5. Next, the chain 61–68 (unbiased for 64–67) is shown.

if the proton distances are less than about 5 Å. Also, the β-proton of Val-39 is the most upfield resonance in the spectrum, which would be consistent with a location in front of the Trp-28 ring, causing an upfield shift.

The solution structure of α-bungarotoxin in the β-sheet around Trp-28 is similar to the X-ray (Walkinshaw et al., 1980) and solution (Kondadkov et al., 1984) structures of the homologous protein α-cobratoxin and to the X-ray structure of the short neurotoxin erabutoxin (Tsernoglou & Petsko, 1976) and is clearly different from the X-ray structure of α-bungarotoxin (Love & Stroud, 1986; Kosen et al., 1988), where Trp-28 lies on the opposite side of the β-sheet. Although models of α-bungarotoxin were built with the region around Trp-28 in the solution or α-cobratoxin conformation, careful refinement of either one, or both molecules within the unit cell in this conformation, showed they were inconsistent with the X-ray data (Love & Stroud, 1986). The density for Trp-28 is visible in Figure 9. Substitution of a valine for the residue at position 36 in X-ray structure of α-cobratoxin, which is equivalent to Val-39 of α-bungarotoxin, by a computer graphics manipulation, demonstrates that if there were a Val-36, it would be right in front of the Trp-25 ring (equivalent to Trp-28 in α-bungarotoxin), as we found in the solution structure of α-bungarotoxin. Figure 10 shows the proximity of these two residues, after this substitution and after rotation of the valine side chain in order to minimize van der Waals contacts between Val-36 and Trp-25. This further demonstrates the similarity between the solution structure of α-bungarotoxin and the X-ray structure of α-cobratoxin.

The β-proton of Val-39 shows a significant temperature dependence of its chemical shift (0.02 ppm/10 °), being at higher field at lower temperatures. A temperature-dependent chemical shift can be attributed to the presence of a minor conformation in fast exchange (Anet & Basus, 1978; Basus, 1975). Thus these observations are consistent with the presence of a minor form with the Trp-28 ring away from Val-39 as observed in the crystal structure. At lower temperatures a smaller amount of this minor form would be present, as dictated by the Boltzmann distribution, and the average chemical shift would be more representative of the major form which has the Val-39 β-proton shifted upfield due to ring current shifts from the Trp-28 ring. This is consistent

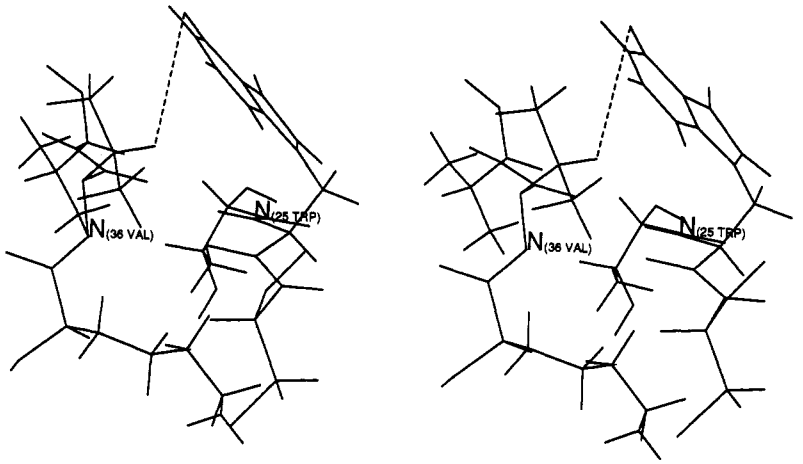

FIGURE 10: Stereopair view of the X-ray structure of α-cobratoxin (Walkinshaw et al., 1980) with Arg-36 changed to valine with side-chain rotation to minimize the van der Waals interactions between the valine side chain and that of Trp-25. The distance indicated by the dotted line is 3.4 Å.

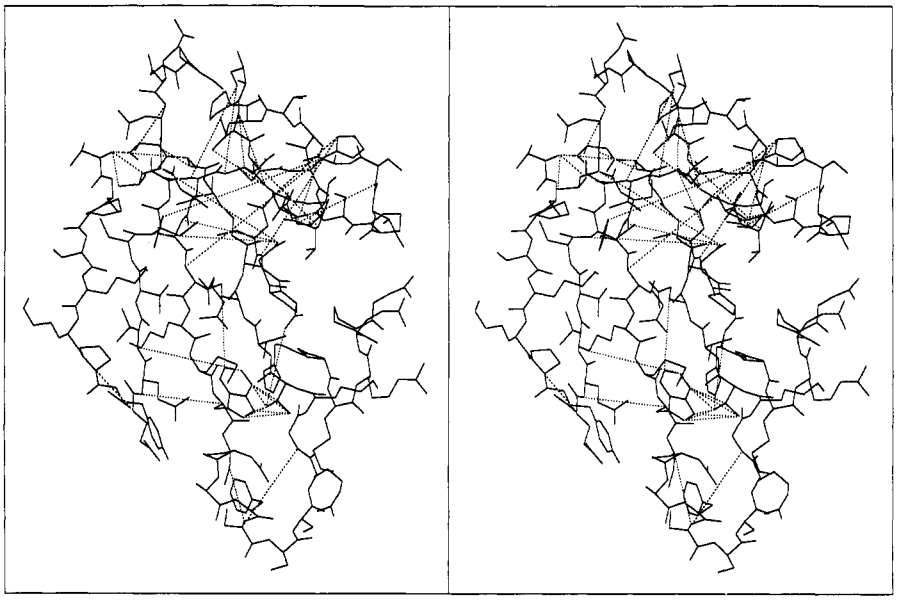

FIGURE 11: Stereopair view of the revised X-ray structure of α-bungarotoxin (Kosen et al., 1988). The dotted lines indicate distances which are in disagreement with the NOEs observed in solution (see Table II).

with the observed shift to higher field at lower temperatures. Thus, this minor form may be more closely related to the structure observed in the crystal.

So far, we have been able to assign only 78 of the 200 long-range (nonsequential) NOE cross-peaks observed in the NOESY spectrum, mainly due to the overlap of resonances within the 0.01 ppm criterion used, although in the range of 1.0–2.2 ppm a larger criterion had to be used due to the complexity of the coupling patterns of the side-chain resonances. Since we must not assume a structure, these cross-peaks must be all uniquely assigned. Many of these have small intensity so that the HRNOESY experiment will not assist in their assignment. Therefore, we must rely on pH and temperature dependence of the chemical shifts to assign uniquely these cross-peaks. While the 78 long-range NOEs now assigned have not been quite enough to give a good structure with distance geometry, a comparison can be made with the revised crystal structure (Kosen et al., 1988). Table II shows the assigned long-range NOEs and the distances obtained from the X-ray structure for comparison. Several distances are in disagreement with the solution structure on the basis of the observation of the corresponding proton to proton NOEs. The maximum distance between two protons giving rise to a detectable NOE in a NOESY spectrum with 160-ms mixing time was estimated on the basis of the NOEs within the Trp-28 ring, by use of a complete relaxation matrix analysis (Keepers & James, 1984) with the program CORMA developed in our laboratory by Dr. Brandan Borgias. With only the tryptophan ring coordinates being used, the observed NOEs at 35 °C were consistent with a 5-ns correlation time. The smallest observable cross-peaks were about equal in intensity to the cross-peak between the ring NH proton and the $C^{\gamma}H$ proton. This distance is 4.9 Å. The intensity of this cross-peak was calculated to have 70% of its intensity from spin diffusion through the $C^{\zeta 2}H$ proton, which is located 2.7 Å from the NH and 2.6 Å from the $C^{\gamma}H$ proton. Since the spin-diffusion contribution would be approximately the same were these protons arranged linearly, we can estimate that for distances greater than 5.3 Å no cross-peaks would be observable at this mixing time even with a spin-diffusion contribution. Thus discrepancies between the X-ray crystal structure and the NMR solution structure are only indicated in Table II for distances in the crystal greater than 5.3 Å. Several were in the 10-Å range, particularly those involving Trp-28 and Val-39, which are clearly different from the solution structure. Figure 11 shows the spatial arrangement of

Table II: Comparison of Distances from the Assigned NOEs (i.e., <5.3 Å) to the Crystal Structure Distances[a]

proton pair for which an NOE is observed	distances found in the crystal structure (Å)	proton pair for which an NOE is observed	distances found in the crystal structure (Å)
$C^{\alpha}H$ Val-40–$C^{\alpha}H$ Met-27	4.99	$C^{\alpha}H$ Lys-26–$C^{\alpha}H$ Val-57	2.00
$C^{\alpha}H$ Leu-42–$C^{\alpha}H$ Arg-25	2.05	$C^{\alpha}H$ Tyr-24–$C^{\alpha}H$ Cys-59	2.84
$C^{\alpha}H$ Cys-44–$C^{\alpha}H$ Cys-23	3.29	$C^{\alpha}H$ Cys-3–NH Lys-64	4.58
$C^{\alpha}H$ Cys-23–NH Ala-45	4.90	$C^{\alpha}H$ Tyr-24–NH Cys-60	2.96
$C^{\alpha}H$ Val-57–NH Met-27	2.99	$C^{\alpha}H$ Thr-5–NH Ala-7	6.41[b]
$C^{\alpha}H$ Lys-26–NH Thr-58	3.50	$C^{\alpha}H$ Cys-59–NH Arg-25	3.62
$C^{\alpha}H$ Cys-44–NH Tyr-24	2.94	$C^{\alpha}H$ Trp-28–NH Glu-56	6.53[b]
$C^{\alpha}H$ Thr-15–NH Cys-3	3.31	$C^{\alpha}H$ Ser-9–NH Ile-11	5.28
$C^{\alpha}H$ Ala-46–NH Asn-21	8.66[b]	$C^{\alpha}H$ Asp-63–NH Val-2	7.88[b]
$C^{\alpha}H$ Asp-63–NH Cys-65	6.54[b]	$C^{\alpha}H$ Ala-45–NH Thr-47	5.52[b]
$C^{\alpha}H$ Cys-33–NH Gly-37	6.03[b]	$C^{\alpha}H$ Pro-53–NH Glu-55	5.54[b]
$C^{\alpha}H$ Lys-64–NH Asn-66	4.16	NH Glu-41–NH Lys-26	3.48
NH Glu-56–NH Met-27	5.26	NH Cys-23–NH Cys-60	3.72
NH Cys-3–NH Thr-6	9.11[b]	NH Ala-45–NH Leu-22	9.97[b]
NH Thr-5–NH Ser-12	4.16	NH Tyr-24–NH Gly-43	3.99
NH Val-2–NH Lys-64	8.29[b]	$C^{\gamma}H_3$ Val-2–NH Lys-64	7.85[b]
$C^{\gamma}H_3$ Thr-5–NH Ala-7	7.56[b]	$C^{\delta}H_3'$ Leu-22–NH Cys-60	5.42
$C^{\delta}H_3$ Leu-22–NH Cys-60	4.25	$C^{\delta}H_3'$ Leu-22–NH Cys-48	4.38
$C^{\delta}H_3$ Leu-22–NH Cys-48	3.67	$C^{\delta}H_3$ Leu-22–NH Ser-61	3.70
$C^{\gamma}H_3$ Val-2–NH Cys-16	3.80	$C^{\gamma}H_3$ Thr-5–NH Val-14	8.88[b]
$C^{\gamma}H_3$ Val-39–NH Trp-28	5.29	$C^{\delta}H_3$ Ile-1–NH Asp-63	7.51[b]
$C^{\gamma}H_3$ Val-39–NH His-68	11.32[b]	$C^{\gamma}H_3$ Thr-5–NH Ser-12	7.20[b]
$C^{\delta}H_3$ Ile-1–NH Thr-62	7.73[b]	$C^{\delta}H_3'$ Leu-22–NH Thr-47	8.55[b]
$C^{\delta}H_3$ Leu-22–NH Thr-47	7.69[b]	$C^{\gamma}H_3$ Val-39–$C^{\delta}H$ Phe-32	5.81
NH Tyr-24–$N^{\delta}H_2$ Asn-66	6.79[b]	NH His-4–$N^{\delta}H_2$ Asn-66	5.18
NH Cys-60–$N^{\delta}H_2$ Asn-66	9.01[b]	NH Ala-45–$C^{\delta}H$ Tyr-24	3.81
NH Asn-66–$C^{\delta}H$ His-4	9.24[b]	NH Gly-43–$N^{\delta}H_2$ Asn-66	4.08
$C^{\alpha}H$ Cys-44–$C^{\delta}H$ Tyr-24	2.94	$C^{\alpha}H$ Leu-22–$N^{\delta}H_2$ Asn-66	9.70[b]
$C^{\alpha}H_2$ Gly-43–$C^{\epsilon}H$ Tyr-24	3.66	NH Lys-26–$C^{\delta}H$ Tyr-24	4.20
$C^{\beta}H_2$ His-4–NH Arg-25	12.75[b]	$C^{\beta}H_2$ Cys-29–NH Cys-33	5.74[b]
$C^{\beta}H_2$ Cys-3–$N^{\delta}H_2$ Asn-66	4.60	$C^{\alpha}H$ Lys-64–$C^{\delta}H$ His-4	6.40[b]
$C^{\beta}H_2$ His-4–$C^{\delta}H$ Tyr-24	13.62[b]	$C^{\epsilon}H_2$ Lys-26–$C^{\eta}H$ Trp-28	13.31[b]
$C^{\beta}H$ Val-39–$C^{\zeta 2}H$ Trp-28	11.84[b]	$C^{\gamma}H_3'$ Val-39–$N^{\epsilon}H$ Trp-28	8.95[b]
$C^{\gamma}H_3'$ Val-39–$C^{\delta}H$ Trp-28	7.71[b]	$C^{\gamma}H_3$ Val-39–$C^{\delta}H$ Trp-28	6.54[b]
$C^{\gamma}H_3$ Val-39–$N^{\epsilon}H$ Trp-28	8.03[b]	$C^{\gamma}H_3'$ Val-39–$C^{\zeta 2}H$ Trp-28	11.17[b]
$C^{\gamma}H_3$ Val-39–$C^{\zeta 2}H$ Trp-28	9.90[b]	$C^{\zeta 3}H$ Trp-28–$C^{\beta}H_2$ Glu-41	9.86[b]
$C^{\delta}H$ Tyr-24–NH Cys-44	3.90	$C^{\epsilon}H$ Tyr-24–NH Lys-26	5.19
$C^{\epsilon}H$ Tyr-24–NH Ala-45	2.68	$C^{\gamma}H_3$ Val-40–$C^{\delta}H$ His-68	4.54
NH Arg-36–NH Cys-33	7.74[b]	$C^{\gamma}H_3$ Val-57–$C^{\delta}H$ Tyr-24	4.53

[a] Proton to proton distances after modeling the best proton locations on the X-ray structure (Kosen et al., 1988). For methyls the distances are to its central carbon, and inconsistencies are indicated only for distances <6.3 Å. [b] Crystal structure distances which are inconsistent with the observed NOEs.

these discrepancies, showing that their distribution is spread to both ends of the β-sheet, and also the first loop from residue 3 to residue 16. The triple-stranded β-sheet region is clearly established in solution. The observed NOEs and hydrogen bonds suggested by the slow amide exchange rates, based on our assignments of the resonances observed in D_2O spectra and the previously reported exchange rates (Endo et al., 1981), indicate that the β-sheet extends farther than it does in the crystal structure (Figure 8). A small rotation of part of the crystal structure would position the carbonyl of Cys-60 to hydrogen bond with the amide group of Cys-23, as found in solution. The other hydrogen bonds detected by NMR could only be formed with more major conformational changes to the X-ray structure, none of which are consistent with the X-ray data. The X-ray structure analysis of α-bungarotoxin was refined at 2.5-Å resolution; thus it is pertinent to ask whether the density could be interpreted in a manner consistent with the solution structure. We sought to test this possiblity especially with respect to His-4, which appears to be far from residues 24–25 (Tyr-24 C^{δ}, Arg-25 N) and 64–66 (Lys-64 C^{α}, Asn-66 N), in the crystal conformation. To determine the reliability in this area, phases were computed by leaving out from one of the two molecules seen in the crystal residues Cys-3, His-4, Thr-5, and Lys-64 through Pro-67, which lie in the electron density that could be close to the His-4 side-chain in solution. A $(2F_o - F_c)$ map (which is essentially an electron density map unbiased by the model) for the region including the omitted residues was calculated and inspected in this region (see Figure 9). Continuous density for the polypeptide throughout the omitted regions returns, indicating their general correctness. There is no electron density at sites which do reconcile with the solution distances. However, features of the map urge some caution in this N-terminal region (Love & Stroud, 1986). Density assigned to the side chain of His-4 returns as strong continuous electron density for all the atoms of the histidine ring, with unresolved atoms as expected at 2.5-Å resolution, however with no density for the β-carbon in this "unbiased" map. The adjacent residue, Cys-3, is in quite strong density, and Cys-3 must be tied closely to Cys-23 in the well-defined β-sheet region, acting as a strong guide post. However, the side chains of the next residue, Thr-5, and Asn-66 are incompletely resolved one from the other, and the peptide bond between Ala-7 and Thr-8 is disordered and not defined in the map. Thus there is a possibility that His-4 could occupy the unresolved density assigned to the side chains of Asn-66 and Thr-5 and might better reconcile with the NMR observations though the distances would still be too large (His-4 C^{β}–Arg-25 NH = 7.5 Å; His-4 C^{β}–Tyr-24 C^{δ} = 9.4 Å). Disadvantages of this assignment (which lead us to doubt it) are also that this would leave the strong density at the current site for the His-4 side chain unexplained and it would place one more whole residue, Thr-6, into the disordered region

at residues 7 and 8. Thus, while continuity and side-chain densities are strong and support the X-ray conformation of His-4, they are not completely unambiguous. The crystal conformation of His-4 lies at a close molecular interface and is close to the N-terminus; thus, the difference from solution conformation here most likely derives from crystal packing.

The differences between the solid-state and solution structures suggest that there is more than one low-energy conformation of α-bungarotoxin and that these structures have different backbone geometry. Furthermore, these must have a relatively low barrier to interconversion since the crystal packing forces are sufficient to bring about such a conformational change or to select a minor conformer. Such flexibility may be necessary for binding to the acetylcholine receptor molecule, which is thought to occur over a large portion of the β-sheet (Low, 1979; Kistler et al., 1982; Love & Stroud, 1986). Also, since neurotoxins must be able to bind to acetylcholine receptor from many species, this flexibility may be necessary functionally to accommodate minor structural differences between receptors from different species.

ACKNOWLEDGMENTS

We thank Dr. Sandasivam Manogaran and Dr. Ruud Scheek for their development of the NMR data processing software, Dr. Brandan Borgias for his assistance with his CORMA program, and Dr. Janet Finer-Moore for her assistance with the X-ray data interpretation. The computer graphics laboratory at UCSF is supported by NIH Grant RR-01081-10 to Dr. Robert Langridge.

Registry No. α-Bungarotoxin, 11032-79-4.

REFERENCES

Agard, D. A., & Stroud, R. M. (1982) *Acta Crystallogr., Sect. A: Cryst. Phys., Diffr., Theor. Gen. Crystallogr. A38*, 186.

Anet, F. A. L., & Basus, V. J. (1978) *J. Magn. Reson. 32*, 339.

Basus, V. J. (1975) Ph.D. Thesis, University of California, Los Angeles.

Basus, V. J. (1984) *J. Magn. Reson. 60*, 138.

Basus, V. J., & Scheek, R. M. (1988) *Biochemistry* (second paper of three in this issue).

Bax, A., & Davis, D. G. (1985) *J. Magn. Reson. 65*, 355.

Billeter, M., Braun, W., & Wüthrich, K. (1982) *J. Mol. Biol. 155*, 321.

Billeter, M., Basus, V. J., & Kuntz, I. D. (1988) *J. Magn. Reson. 76*, 400.

Dufton, M. J., & Hider, R. C. (1983) *CRC Crit. Rev. Biochem. 14*, 113.

Endo, T., Inagaki, F., Hayashi, K., & Miyazawa, T. (1981) *Eur. J. Biochem. 120*, 117.

Inagaki, F., Hider, R. C., Hodges, S. J., & Drake, A. F. (1985) *J. Mol. Biol. 183*, 575.

Karlsson, E. (1979) *Handb. Exp. Pharmacol. 52*, 159–212.

Keepers, J. W., & James, T. L. (1984) *J. Magn. Reson. 57*, 404.

Kistler, J., Stroud, R. M., Klymkowsky, M. W., Lalancette, R. A., & Fairclough, R. H. (1982) *Biophys. J. 37*, 371.

Kondakov, V. I., Arseniev, A. S., Pluzhnikov, K. A., Tsetlin, V. I., Bystrov, V. F., & Ivanov, V. T. (1984) *Bioorg. Khim. 10*, 1606.

Kosen, P. A., Finer-Moore, J., McCarthy, M. P., & Basus, V. J. (1988) *Biochemistry* (third paper of three in this issue).

Love, R. A., & Stroud, M. (1986) *Protein Eng. 1*, 37.

Low, B. W. (1979) *Handb. Exp. Pharmacol. 52*, 213–257.

Marion, D., & Wüthrich, K. (1983) *Biochem. Biophys. Res. Commun. 113*, 967.

Mebs, D., Narita, K., Inagawa, S., Samegima, Y., & Lee, C. Y. (1971) *Biochem. Biophys. Res. Commun. 44*, 711.

Nagayama, K., & Wüthrich, K. (1981) *Eur. J. Biochem. 114*, 365.

Pearson, G. A. (1977) *J. Magn. Reson. 27*, 265.

Piantini, O. W., Sørensen, O. W., & Ernst, R. R. (1982) *J. Am. Chem. Soc. 104*, 6800.

Rance, M., Sørensen, O. W., Bodenhausen, G., Wagner, G., Ernst, R. R., & Wüthrich, K. (1984) *Biochem. Biophys. Res. Commun. 117*, 479.

Redfield, A. G., & Kuntz, S. D. (1975) *J. Magn. Reson. 19*, 250.

Shaka, A. J., & Freeman, R. (1983) *J. Magn. Reson. 51*, 169.

States, D. J., Haberkorn, R. A., & Ruben (1982) *J. Magn. Reson. 48*, 286.

Tsernoglou, D., & Petsko, G. A. (1976) *FEBS Lett. 68*, 1.

Wagner, G., & Wüthrich, K. (1982) *J. Mol. Biol. 155*, 347.

Walkinshaw, M. D., Saenger, W., & Maelicke, A. (1980) *Proc. Natl. Acad. Sci. U.S.A. 77*, 2400.

Wider, G., Lee, K. H., & Wüthrich, K. (1982) *J. Mol. Biol. 155*, 367.

Wüthrich, K., Wider, G., Wagner, G., & Braun, W. (1982) *J. Mol. Biol. 155*, 319.

Wüthrich, K., Billeter, M., & Braun, W. (1984) *J. Mol. Biol. 180*, 715.